Controlled fabrication of hierarchically branched nanopores, nanotubes, and nanowires

Guowen Meng*, Yung Joon Jung*, Anyuan Cao*, Robert Vajtai*†, and Pulickel M. Ajayan*‡

*Department of Materials Science and Engineering and †Rensselaer Nanotechnology Center, Rensselaer Polytechnic Institute, Troy, NY 12180

Communicated by Bruce Watson, Rensselaer Polytechnic Institute, Troy, NY, March 14, 2005 (received for review January 18, 2005)

Here, we report a generic synthetic approach to rationally design multiply connected and hierarchically branched nanopores inside anodic aluminum oxide templates. By using these nanochannels, we controllably fabricate a large variety of branched nanostructures, far more complex than what exists today. These nanostructures include carbon nanotubes and metallic nanowires having several hierarchical levels of multiple branching. The number and frequency of branching, dimensions, and the overall architecture are controlled precisely through pore design and templated assembly. The technique provides a powerful approach to produce nanostructures of greater morphological complexity, which could have far-reaching implications in the design of future nanoscale systems.

The design and controlled synthesis of complex nanowire (1–5) and carbon nanotubes (CNTs) (6–8) will impact developments in nanotechnology applications. The present synthesis approaches, however, limit the degree of complexity that can be controllably configured into these structures. Fabrication inside rationally designed porous templates [such as anodic aluminum oxide (AAO) templates] is ideal to produce nanowire morphologies, but this feat has been accomplished controllably only for linear (9–15) and Y-shaped (6, 7) architectures. The creation of controlled pore structure, with various levels of complexity, inside these templates provides a powerful way to produce predesigned multiply connected and branched nanowires and nanotubes. We have developed a rational approach for creating hierarchically branched nanoporous AAO templates and have fabricated a whole generation of branched nanowires and nanotubes inside these templates. As a suitable example, we detail the case of CNT structures in this work, but other material systems can also be made into similar architectures, as highlighted for the case of metallic nanowires in *Materials and Methods.*

Materials and Methods

Preparation of AAO Templates. AAO templates were prepared by using a modified two-step anodization process (6, 16). The first-step anodization was the same for all templates. High-purity Al foils were anodized in 0.3 M oxalic acid solution at 8–10°C under a constant voltage (in the range of 40–72 V_{dc}) for 8 h. Then, the formed anodic aluminum layer was removed. In the second-step anodization, templates with different pore architectures underwent different processes of anodization as follows.

AAO Templates with Multiple Generations of Y-Branched Pores. We reduced the anodizing voltage multiple times in the second-step anodization. Initially, the anodization was performed under the same conditions as those in the first step to create the primary stem pores; then, the anodizing voltage was reduced by a factor of $1/\sqrt{2}$ to form Y-branched pores. Two-, three-, and four-generation Y-branched pores can be obtained by further sequential reduction of anodizing voltages. It is noted that if a subsequent anodizing voltage is ≤25 V, after any prior anodization, the samples should be washed in deionized water for ≈30 min to clean the remaining oxalic acid solution in the pores, and then the anodization should be conducted in 0.3 M sulfuric acid at the same temperature used previously.

AAO Templates with Multiply Branched Pore Structure. After the initial anodization to form the stem pores, the anodizing voltage was reduced by a factor of $1/\sqrt{n}$ to create multiply branched (n branches) pores. If the voltage is reduced slowly, the stem pores divide branched pores gradually (at several depths), but if the voltage is reduced suddenly, the stem pores will be divided abruptly (sharp interface). Typically, after the anodization for the stem pores, we cleaned the remaining oxalic acid solution in the pores in deionized water and thinned the barrier layer at the pore bottom by immersing the samples in a 5% (wt) phosphoric acid solution at 31°C for 30–70 min. It should also be noted that if the anodizing voltage for branched pores is ≤25 V, a 0.3-M sulfuric acid electrolyte should be used instead of oxalic acid.

AAO Templates with Several Levels of Multiply Branched Pores. After the initial anodization for primary stem pores, the anodizing voltage was reduced by a factor of $1/\sqrt{n}$ to create first-generation multibranched (n) pores, and we subsequently reduced the anodizing voltage again by a factor of $1/\sqrt{m}$ to generate the second-generation multibranched pores growing from each of the first-generation multibranched pores.

Growth of Carbon Nanotubes in AAO Template. Multiwalled nanotubes were grown inside the pores of the AAO templates by the pyrolysis of acetylene (6, 12, 13) at 650°C for 1–2 h with a flow of gas mixture of Ar (85%) and C_2H_2 (15%) at a rate of 35 ml/min.

Electrochemical Deposition of Ni Nanowires in AAO Template. After the final anodization, the remaining Al layer at the bottom of AAO templates was removed in a saturated $SnCl_4$ solution. Before removing the barrier layer, the top surface of the templates was covered with nail polish to protect the pores if the barrier layer was thinned before the anodization for the branched pores. An adhesion layer of Ti (10 nm) and Cu film (1 μm) was coated onto the stem pore side of the AAO templates by electron-beam evaporation to cover the pores completely and to serve as the working electrode in electrochemical deposition. Ni nanowires were electrodeposited into the pores of AAO templates by using standard procedures (17).

Template Removal. Nanotubes were released from AAO templates by dissolving the templates in a 20% (wt) HF solution for 12 h, and then washed with deionized water several times. Ni nanowires were released from AAO templates by immersing the samples in a 10% (wt) NaOH solution for 1 h, and then washed with deionized water several times.

Abbreviations: AAO, anodic aluminum oxide; CNT, carbon nanotube.

‡To whom correspondence should be addressed. E-mail: ajayan@rpi.edu.

www.pnas.org/cgi/doi/10.1073/pnas.0502098102

Details of Diameter Evolution. The pore diameter developed inside the template depends on the following three processes.

1. For the anodization process, based on previous work (18–21), the pore diameter is proportional to the anodizing voltage, and the diameter attributed by the anodization can be expressed as $D = \kappa \times V\,(nm)$, where V refers to the anodizing voltage, and κ is a constant (nmV^{-1}) as reported previously.
2. Thinning the barrier layer process before further anodization for multibranched pores also widens the existing pores; the diameter increase depends on the pore widening rate and thinning barrier layer time.
3. Removing the barrier layer in the final process of template preparation also will increase the pore diameter if the top surface is not covered with nail polish. The diameter increase depends on the pore widening rate and removing barrier layer time.

Templates with different pore structures undergo different processes, so the final diameters of the pores (and correspondingly, the outer diameter of nanotubes grown) in different structured templates can be calculated separately.

The diameter ratios of the nanotube structures (ratio of the smallest diameter to the stem diameter created) that are produced experimentally are given in Table 1, which is published as supporting information on the PNAS web site. Both theoretically calculated ratios and experimentally observed values are shown, and there is an excellent correspondence between the two.

Results

Fig. 1 shows the schematic of the fabrication process and the different architectures that we have synthesized for CNTs using these templates. Such a wide range of complex nanopore, nanotube, and nanowire structures, with multiple junctions and branches, has never before been built, to our knowledge. To denote this broad spectrum of architectures with multiple levels of branching, we introduce the notation $\boldsymbol{1 \prec n \prec m}$, where "$\prec$" stands for the junction where the branching takes place, and $\boldsymbol{n}$ or $\boldsymbol{m}$ stands for the number of branches produced; the simplest case of a Y-junction thus is denoted as a $\boldsymbol{1 \prec 2}$ structure.

First, we extended the rationale for creating Y-branched pores in AAO templates (6) by reducing the anodizing voltage by a factor of $1/\sqrt{2}$, which initiates the transformation of a linear pore during anodization into a symmetrically divided Y. Based on this rationale, we show that it is possible to generate not just a single Y junction but multiple generations of Y-branching by sequentially reducing the anodizing voltage multiple times, each time by the factor of $1/\sqrt{2}$. Once the complex pore structure is generated, the template is ready to be used to grow the representative nanotube or nanowire structures. The nanotubes are deposited inside the pores by the pyrolysis of acetylene (6, 12, 13) without the use of any catalyst material. The nanotubes grown here are multiwalled (≈4–10 walls), have a diameter range of ≈20–120 nm, and are graphitic in nature. Once the nanotubes are grown inside the templates, the templates can be removed by etching the alumina away to obtain isolated nanotubes and their arrays. From our observations of several branched multiwalled nanotube structures, presented below, the wall thickness (and hence the number of walls) falls within a very narrow range of ≈1–4 nm. We normally observe small reduction in the number of walls (approximately two or three walls) as a larger tube changes into smaller ones, and this reduction seems to happen quite abruptly.

Up to four generations of Y-branching have been fabricated onto individual nanotube structures ($\boldsymbol{1 \prec 2 \prec 2 \prec 2 \prec 2}$), as shown in Fig. 2 in the scanning electron microscope (SEM) images. Fig. 2*A Right* shows the architecture of each of the nanotube formed inside the template. Fig. 2*A Left* shows the four parallel interfaces (arrows), seen in a large bundle of nanotubes obtained after template removal, where each of the four generations of Y-branching takes place. The high-magnification image from each of these interfaces (Fig. 2 *B–E*) clearly reveals the corresponding Y-branches. The diameters of the primary stems and the branches depend on the corresponding anodizing voltages; for any two consecutive branches (at each interface), the ratio of the diameters is approximately $\sqrt{2}$, as seen from the figures (the details of diameter evolution during anodization at different voltages is provided in Table 1 and in *Materials and Methods*). The diameter ratios of the smallest branch and the primary stem in several of the architectures that we have fabricated are presented in Fig. 1. The length of each branch is controlled independently by the corresponding anodization time given for each pore segment generation.

Next, we generated templates where the individual pores divide into predetermined multiple numbers of branches. This process

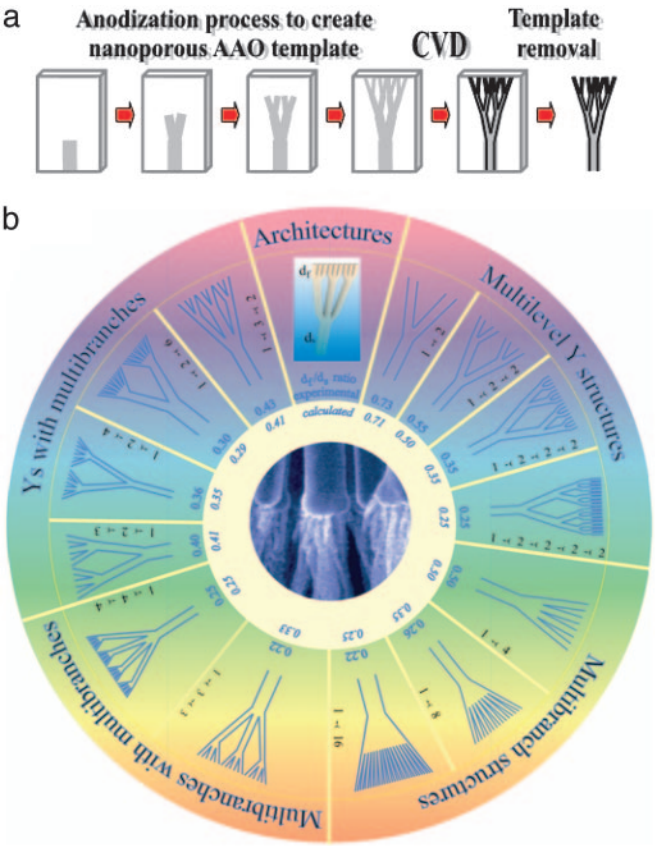

Fig. 1. Schematics of fabrication process and the resulting branched nanowire structures. (*a*) Schematic showing the synthesis process, where the pores with controlled architectures are first developed inside the template (by consecutive steps of anodization) and then used as molds to cast nanotubes and nanowires of complex geometries. The templates then are removed by etching to recover the structures. (*b*) Schematic showing a catalog of CNT architectures that are controllably fabricated within the nanoporous AAO templates. The structures are categorized in the schematic based on four different hierarchies of branching of stems: multiple generations of Y-branching from one stem, multiple branching from individual stems, combination of Y-branching with each branch undergoing multiple-branching (or reverse), and a combination of multiple branching with each branch developing multiple branches. Examples of structures, which have been experimentally made, are drawn in the schematic. As seen in the drawings, the diameter of the nanotube stems progressively decrease as the branching continues and these diameters are theoretically related to the ratios of the anodizing voltages consecutively used to divide pores inside the AAO. The theoretical values of the diameter ratios (smallest to largest diameter on each structure) are shown by the fractional numbers in each of the sectors and compared with the measured values.

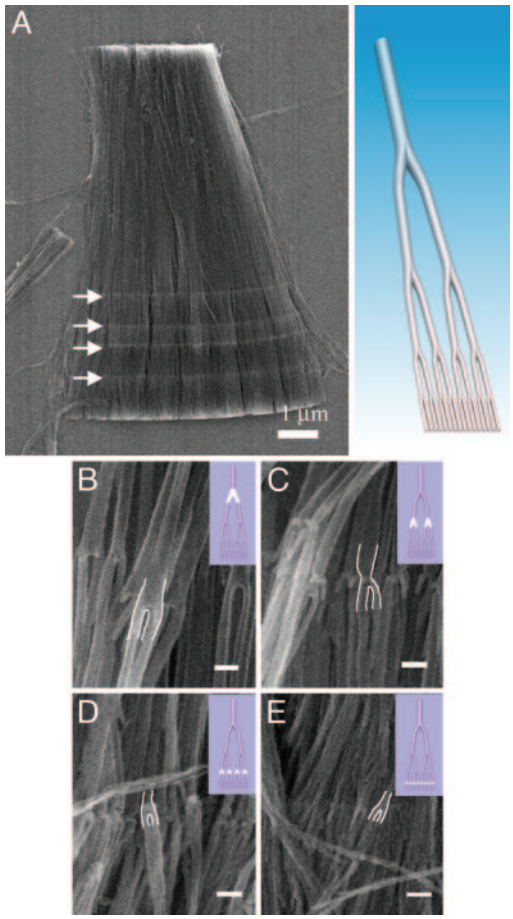

Fig. 2. CNT architectures showing four-generation Y-branching. (*A*) Drawing (*Right*) shows the structure of the typical four-generation Y-branched nanotube. (*Left*) The four parallel interfaces (marked with white arrows) in the low-magnification SEM image show the locations where the four generations of Y-branching take place, respectively. (*B–E*) The high-magnification image from each interface clearly reveals the corresponding Y-branches and the decreasing diameters of the branched nanotube segments, showing the first (*B*), second (*C*), third (*D*), and fourth (*E*) Y generations. The Y-junction is contoured in white lines for clarity. *Insets* at top right show schematics of the whole architecture with the specific junction highlighted in white. (Scale bars: 100 nm.)

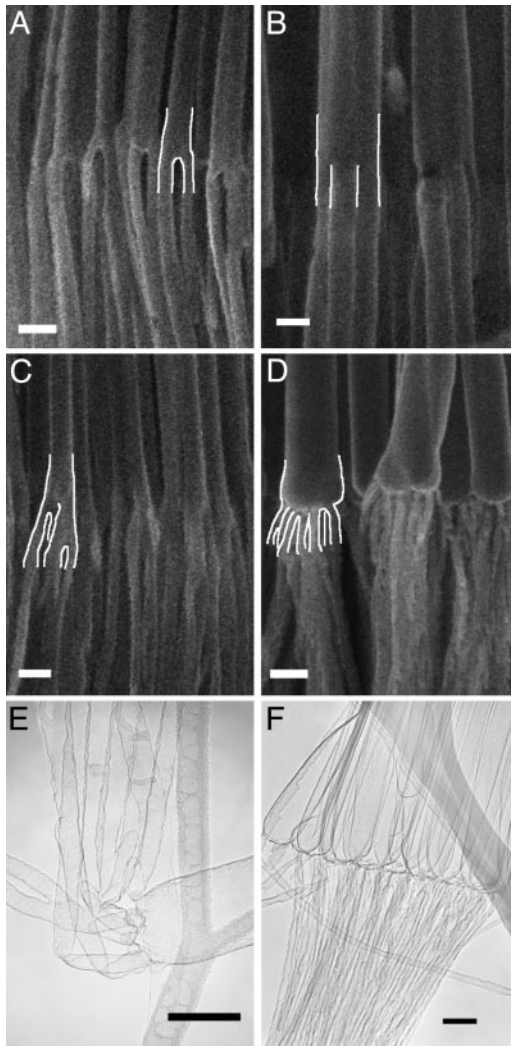

Fig. 3. CNT architectures showing multiple branching. Series of SEM images of multiply branched CNTs showing the primary stem abruptly dividing into 2 (*A*), 3 (*B*), 4 (*C*), and 16 (*D*) branches, respectively. The junctions are highlighted with white line contours for clarity. In the case of the 16-branched nanotube, only half the branches are visible in the image (due to the 3D structure, the rest of the branches are behind the front visible ones). (*E*) A transmission EM image of a nanotube with eight branches. The smaller branches look more flexible and are seen easily bent. (*F*) Transmission EM image from an array of multi-branched (16 branches on each) CNTs. (Scale bars: 100 nm.)

allows us to grow nanotubes and nanowires with predetermined numbers of branches. As the pore diameter is proportional to the anodizing voltage (18–21), so the anodizing voltage controls the pore size and pore density during the anodization. A simple calculation (based on the fact that the original total area of the template will not change during the anodization) shows that the anodizing voltage to form a number of (n) smaller pores from a single stem pore can be expressed as $(1/\sqrt{n}) \times V_s$, where V_s is the anodizing voltage for stem pores, and n is the number of branched pores from that stem. Based on this rationale, we have successfully prepared AAO templates with different numbers of branches emanating from individual pores and grown nanotubes in them. Once again, the precise location (depth) inside the template where the branching occurs is controlled by the sequence and timing of voltage reduction, and the branching can be made to occur abruptly or gradually based on the voltage-reduction procedure. Fig. 3 *A–D* shows nanotubes where a single stem abruptly divides into 2, 3, 4, and 16 (structures ***1*** $\prec$ ***2***, ***1*** $\prec$ ***3***, ***1*** $\prec$ ***4***, and ***1*** $\prec$ ***16***) branches, respectively. We have been able to controllably produce branching numbers at will, for example, 2, 3, 4, 6, 8, and 16. The stem pore diameter mainly depends on the anodizing voltage; however, an intermediate procedure necessary to go from higher to lower anodizing voltages widens the stem pore diameters (seen in several images in Fig. 3; see also Table 1 and *Materials and Methods*). The predicted diameters for the stems and branches come close to experimentally measured values (see Fig. 1 schematic for the experimental and calculated diameter ratios). Also, shown in Fig. 3 *E* and *F* are the transmission EM images of the branched nanotubes, clearly showing the junctions between the larger and smaller nanotubes and the flexibility of the smaller nanotubes (Fig. 3*E*).

A combination of Y-shapes and multiple branches can lead to a wealth of new nanoscale architectures. This goal can be achieved by reducing the anodizing voltages in steps, by factors of $1/\sqrt{2}$ and $1/\sqrt{n}$ sequentially, generating Y-shapes and n-branched pores in the template consecutively. The sequences can be interchangeable (for example, the stem can be split into multiple branches first, and each of the branches can subdivide as Y-shapes or vice versa) and recurring (several levels) so that

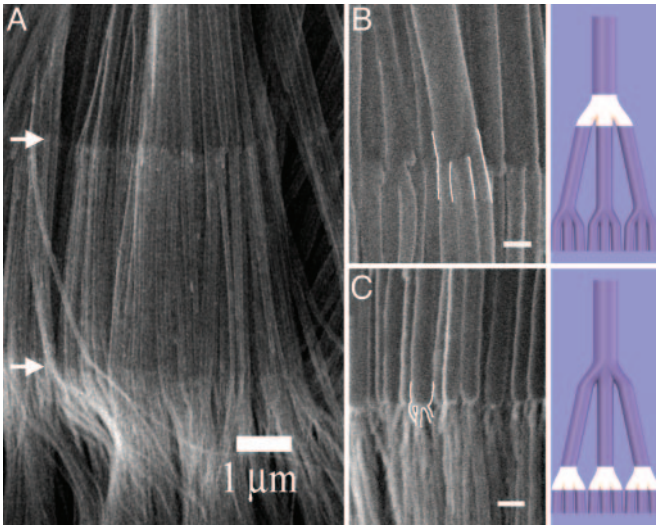

Fig. 4. CNT architectures that have complex hierarchical branching. (*A*) SEM images show arrays of nanotubes that show two generations of branching (at the locations of the white arrows). At each of the junctions each of the stems split into three, giving a ***1*** ≺ ***3*** ≺ ***3*** architecture, as discussed in the text. (*B Left* and *C Left*) Close-up views of the ***1*** ≺ ***3*** junctions. (*B Right* and *C Right*) Schematic of each of the representative individual nanotube structures. Junctions are highlighted with white line contours for clarity. (Scale bars: 100 nm.)

many complicated nanostructures become possible (Fig. 1; catalog of structures). Continuing this approach, very complicated architectures, such as a single stem dividing into multiple branches and each of those branches further subdividing into multiple ((***1*** ≺ ***n*** ≺ ***m***) structures, where ***n*** and ***m*** can be independently varied) can be created. Fig. 4 shows an example of such a complex structure, where two levels of multiple branching are shown (arrows in Fig. 4*A* indicate the interfaces at which branching takes place). The primary stem splits first into three branches, each of which further splits into three subbranches (***1*** ≺ ***3*** ≺ ***3***). The high-magnification SEM images of the two interfaces reveal the junctions, showing the branching and the reduction in diameters as the branching occurs. We have so far made several fascinating structures such as those illustrated in Fig. 1*b* catalog. Some of these architectures also are shown in Figs. 5 and 6, which are published as supporting information on the PNAS web site (see also *Materials and Methods*), in addition to the ***1*** ≺ ***3*** ≺ ***3*** shown in Fig. 4.

By using the templates with tailored pores, we also have grown nanowires in addition to CNTs showing that our approach serves as a generic method for creating complex nanowires of most materials that can either be deposited by means of vapor phase deposition (6, 12, 13) or electrodeposition (9, 10, 14, 15, 21). Some of the complex Ni nanowires generated by this method are shown in Figs. 7 and 8, which are published as supporting information on the PNAS web site (e.g., Ni nanowires of ***1*** ≺ ***2*** ≺ ***2*** and ***1*** ≺ ***4*** types). Insulating, semiconducting, and polymeric materials also may be controllably synthesized into the complex nanowires by using the above templates with infiltration processes described in the literature (9, 10, 14, 15, 22, 23). In addition to single-component nanowire architectures, it also should be possible to make hetero-nanowire junctions, for example by electrodepositing metal in the stems and then growing nanotubes as the branches. The question of growing single-walled nanotubes in these pores also can be addressed. Typically, the smallest pore sizes that can be developed using AAO templates is ≈10 nm, which is much greater than a single-walled nanotube diameter. However, the nanotubes made in the pores have very few walls, and, theoretically, the number of walls may be controlled (to a single layer) by controlling the deposition time. Alternatively, individual or single-walled nanotube bundles may be deposited by seeding small catalyst particles within (or at the bottom of) the pores.

Discussion

In conclusion, we have demonstrated a powerful, rational, synthetic approach for the design and fabrication of hierarchical nanopore/nanotube/nanowire architectures. These are, to our knowledge, the first reported results in the controlled fabrication of complex geometries of nanotubes and nanowires with several levels of junctions and branching and are clear demonstrations of what can be accomplished in architecture building of 1D nanoscale building blocks. The nanopore architectures we have developed are unique, particularly given the control in designing select hierarchies of branched pores, and should complement materials such as zeolites that contain interconnected ordered pore frameworks of different dimensionality, chemistry, and structure (24).

These structures we have described above should open up new opportunities for both fundamental research and building of various nanoscale architectures for applications. The hierarchically branched nanotube/nanowire constructs with tree-like morphology could impart similar functions as polymer dendrimers, which are used to build large supramolecular constructs for applications such as drug delivery (25); e.g., the individual branches here can be differentially chemically functionalized and terminated to create complex multiple chemical sensors in one unit. Such constructs also can be the core structure to build complex nanoscale biomaterials. The multiply branched nanotube/nanowire architectures could be key to building components of complex nanoelectronics circuits (6, 7, 10, 17) and nanoelectromechanical systems (26). The ordered straight pore arrays of traditional AAO templates have been used effectively to build flow-through-type DNA arrays (27); the structures with hierarchically branched nanopores would have interesting applications in such biotechnology applications as nanoscale separation technologies and in fundamental diffusion studies where the multiply divided pores can act as selective barriers in a multicomponent diffusion process.

This work was supported by the Rensselaer Polytechnic Institute, the Interconnect Focus Center New York at Rensselaer Polytechnic Institute, and the National Science Foundation Nanoscale Science and Engineering Center. G.M., who is on leave from the Institute of Solid State Physics (Chinese Academy of Science, Hefei, China), was supported by the Chinese Academy of Science, Natural Science Foundation of China, and Ministry of Science and Technology of China.

1. Milliron, D. J., Hughes, S. M., Cui, Y., Manna, L., Li, J. B., Wang, L. W. & Alivisatos, A. P. (2004) *Nature* **430,** 190–195.
2. Dick, K. A., Deppert, K., Larsson, M. W., Martensson, T., Seifert, W., Wallenberg, L. R. & Samuelson, L. (2004) *Nat. Mater.* **3,** 380–384.
3. Wang, D. L., Qian, F., Yang, C., Zhong, Z. H. & Lieber, C. M. (2004) *Nano Lett.* **4,** 871–874.
4. Xia, Y., Yang, P. D., Sun, Y. G., Wu, Y. Y., Mayers, B., Gates, B., Yin, Y. D., Kim, F. & Yan, Y. Q. (2003) *Adv. Mater.* **15,** 353–389.
5. Wang, Z. L. (2004) *J. Phys. Condens. Matter* **16,** R829–R858.
6. Li, J., Papadopoulos, C. & Xu, J. (1999) *Nature* **402,** 253–254.
7. Papadopoulos, C., Rakitin, A., Li, J., Vedeneev, A. S. & Xu, J. M. (2000) *Phys. Rev. Lett.* **85,** 3476–3479.
8. Dresselhaus, M. S., Dresselhaus, G. & Avouris, P., eds. (2001) *Carbon Nanotubes: Synthesis, Structure, Properties, and Applications* (Springer, New York).
9. Martin, C. R. (1994) *Science* **266,** 1961–1966.
10. Routkevitch, D., Tager, A. A., Haruyama, J., Almawlawi, D., Moskovits, M. & Xu, J. M. (1996) *IEEE Trans. Electron Devices* **43,** 1646–1658.
11. Zhang, Z., Ying, J. Y. & Dresselhaus, M. S. (1998) *J. Mater. Res.* **13,** 1745–1748.
12. Davydov, D. N., Sattari, P. A., AlMawlawi, D., Osika, A., Haslett, T. L. & Moskovits, M. (1999) *J. Appl. Phys.* **86,** 3983–3987.

ENGINEERING

13. Sui, Y.C., Cui, B.Z., Martínez, L., Perez, R. & Sellmyer, D. J. (2002) *Thin Solid Films* **406,** 64–69.
14. Huczko, A. (2000) *Appl. Phys. A* **70,** 365–376.
15. Schmid, G. (2002) *J. Mater. Chem.* **12,** 1231–1238.
16. Masuda, H. & Satoh, M. (1996) *Jpn. J. Appl. Phys. Lett.* **35,** L126–L129.
17. Whitney, T. M., Jiang, J. S., Searson, P. C. & Chien, C. L. (1993) *Science* **261,** 1316–1319.
18. O'Sullivan, J. P. & Wood, G. C. (1970) *Proc. R. Soc. London A* **317,** 511–543.
19. Furneaux, R. C., Rigby, W. R. & Davidson, A. P. (1989) *Nature* **337,** 147–149.
20. Broughton, J. & Davies, G. A. (1995) *J. Membr. Sci.* **106,** 89–101.
21. Choi, J., Sauer, G., Nielsch, K., Wehrspohn, R. B. & Gösele, U. (2003) *Chem. Mater.* **15,** 776–779.
22. Kovtyukhova, N., Mallouk, T. E. & Mayer, T. (2003) *Adv. Mater.* **15,** 780–785.
23. Park, S., Lim, J. H., Chung, S. W. & Mirkin, C. A. (2004) *Science* **303,** 348–351.
24. Treacy, M. M. J. (2003) *J. Microporous Mesoporous Mater.* **58,** 1–2.
25. Patri, A. K., Majoros, I. J. & Baker, J. R. (2002) *Curr. Opin. Chem. Biol.* **6,** 466–471.
26. Srivastava, D., Menon, M. & Cho, K. (2001) *Comput. Sci. Eng.* **3,** 42–54.
27. Matsumoto, K., Nishio, K. & Masuda, H. (2004) *Adv. Mater.* **16,** 2105–2108.